A 50-kW Bidirectional Step-up / Step-down DC/DC Oak Ridge Converter for Wireless Charger Applications

Erdem Asa[1], Omer C. Onar[1], Veda P. Galigekere[1], Gui-Jia Su[1], Burak Ozpineci[1], and Kerim Colak[2]
[1]Oak Ridge National Laboratory, National Transportation Research Center, Tennessee, USA
[2]Hevo Power Inc., New York, USA
E-mail: asae@ornl.com

***Abstract*— This study presents a novel bidirectional concept by using Oak Ridge Converter (ORC) for wireless energy conversion (WEC) technologies such as wireless electric vehicle (EV) chargers, wireless mobile or energy storage systems (MESS / ESS), etc. The presented system can be deployed in a bidirectional wireless power transfer (WPT) structure for different input voltages by using two different operating frequencies. The proposed concept here achieves zero voltage switching (ZVS) in during step-up and step-down configurations. The system overall theoretical design and experimental test results are presented for 50 kW power transfer in both bidirectional operations modes. The laboratory demonstration of the system is presented for the three-phase bidirectional system with 6 inches of airgap between the coils and output of 560 V_{DC} with 95.4% dc-to-dc efficiency.**

Keywords— Oak Ridge Converter, resonant, converter, high frequency, wireless power transfer, bidirectional, step-up / step-down converter

I. INTRODUCTION

Wireless energy conversion systems require bi-directional operation to obtain fully autonomous functionality for an application such as electric vehicles (EVs) or energy storage systems (ESSs) [1]. Bidirectional operation is essential to provide grid ancillary or grid support services systems that amount of energy drawn from the grid is adjusted to increase grid stability and balance the consumption and generation by communicating with the battery charging equipment to manage the load side demand [2]. To increase penetration of renewable energy sources, distributed ESSs can be integrated to the grid by proper energy conversion systems between grid and resources to supplement distributed grid source management [3]-[4]. Bidirectional WPT solutions can offer fully autonomous and customer friendly features and improved safety in severe environmental circumstances and harsh weather conditions for emergency power systems than plug-in charging technologies [5].

In [6]-[8], resonant compensation circuits were investigated using various control strategies for bidirectional WPT applications. The literature investigated single [9] and three-phase bidirectional matrix converter architectures [10] for converting 50-60 Hz ac grid voltage into high frequency voltage. Despite the fact that matrix converter structure eliminates the dc link, their design is sophisticated, and their circuit operation is difficult to configure by controller. WPT systems were also examined using single stage integrated bidirectional ac to dc conversion architectures [11], [12]. In spite of the lower total system cost due to the single switch topology, this converter is prone to high voltage or current stresses, which may result in increased switching power losses. The authors of [13] introduced bidirectional ac/ac converter topology that can be used for power transfer from grid to produce envelope high frequency current on the transmitter side of WPT system. In [14], a bidirectional dc to ac current sourced WPT system architecture between the grid and dc loads was studied.

This study performs a bidirectional step-up/step-down capable ORC converter, ORNL's patented technology [15], in dc/dc operation mode for WPT systems to support multiple interfaces between grid and battery loads such as MESS, ESS, EV batteries, etc. In this technology, bidirectional operation with step-up and step-down functionalities can be achieved by two different operating frequencies providing ZVS operation in both conditions. This simple technology can ensure a unique solution by integrating the different sources in a bidirectional operation for WPT systems. To validate the functionality of the proposed

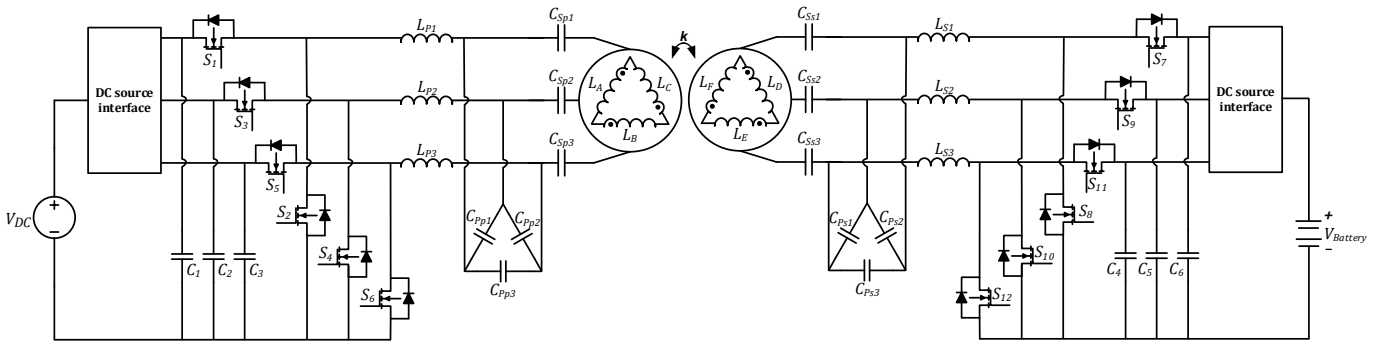

Fig. 1. The illustration of 50kW bidirectional wireless power transfer system.

architecture, the mathematical model examination of the conversion system is established by describing the designed structure. The system experimental performance results are presented at 50 kW with step-up and step-down functionality for an output of 560 V_{DC} and an efficiency of 95.4%.

II. Bidirectional WPT System

The presented bidirectional step-up/step-down WPT system is illustrated in Fig. 1. The designed architecture allows transferring the power between dc source and dc load terminals considering the voltage gain function in bidirectional operation. Furthermore, this system can be used to integrate the different sources wirelessly through the dc interface system such as ESS, MESS, and EV batteries. This purpose of model is individually useful for the use of power conversion system instead of using multiple power conversion / inverter system design, providing design cost reduction to the applications.

As shown in Fig. 1, the system comprises three phase-leg MOSFET power modules, a pair of delta connected three-phase coupling coils with *LCC-LCC* resonant tuning compensation, and the secondary side controllable switches that are three phase-leg power modules. During the battery discharging mode, power is returned back to the source, and secondary side controllable switches operate as a three-phase high frequency inverter. The battery or source can either charge or discharge the energy in both power flow directions. The single-phase corresponding equal circuit and simplified diagrams of the resonant network with the coupler coils are given in Fig. 2 (a) and Fig. 2 (b), respectively.

In a matrix form, the coupler primary and secondary inductances L_P, L_S can be represented as,

$$L_P = \begin{bmatrix} L_A & M_{AB} & M_{CA} \\ M_{AB} & L_B & M_{BC} \\ M_{CA} & M_{BC} & L_C \end{bmatrix},\ L_S = \begin{bmatrix} L_D & M_{DE} & M_{FD} \\ M_{DE} & L_E & M_{EF} \\ M_{FD} & M_{EF} & L_F \end{bmatrix} \quad (1)$$

where L_A, L_B, L_C are primary-side self-inductances and L_D, L_E, L_F are secondary-side self-inductances. Also, M_{AB}, M_{BC}, M_{CA} and M_{DE}, M_{EF}, and M_{FD} represent mutual inductances between primary phases L_A and L_B, L_B and L_C, L_C and L_A, and secondary phases L_D and L_E, L_E and L_F, L_F and L_D, respectively.

(a)

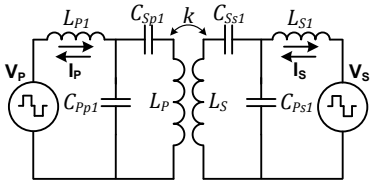

(b)

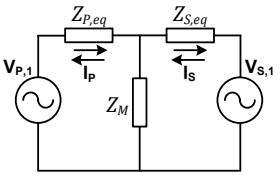

Fig. 2. Bidirectional *LCC-LCC* resonat network of the wireless power transfer system; single phase equiavalent diagram (a) and single phase simplified diagram (b).

The series resonant tuning inductors L_{Ps}=L_{Ps1}=L_{Ps2}=L_{Ps3} can be calculated as,

$$L_{Ps} = \frac{V_{P,max}}{\pi(2\pi f_{sw})I_P} = \frac{3\eta}{\pi^2(2\pi f_{sw})}\frac{V_{P,max}^2}{P_O} \quad (2)$$

where $V_{P,max}$ is the maximum input phase voltages, P_O is the the average total output power, η is the overall system efficiency, and f_{sw} is the operating frequency of the resonant network. The values of the delta connected parallel compensation capacitors C_{Pp}=C_{Pp1}=C_{Pp2}=C_{Pp3} and the series compensation capacitors C_{Ps}=C_{Ps1}=C_{Ps2}=C_{Ps3} can be expressed by,

$$C_{Pp} = \frac{1}{3(2\pi f_{sw})^2 L_{Ps}} \quad (3)$$

$$C_{Ps} = \frac{1}{(2\pi f_{sw})^2(L_P/3 - L_{Ps})} \quad (4)$$

The presented technology is symmetrical and primary side parameters are uniform with the secondary side parameters. Hence, defined resonant compensation specifications can be characterized same as in the secondary side. The *LCC-LCC* compensation network components deployed in this topology are specified in Table I, where the primary side components L_{Ps},

C_{Pp}, C_{Ps}, L_P, and the secondary components L_{Ss}, C_{Sp}, C_{Ss}, L_S, respectively.

TABLE I – CALCULATED RESONANT TANK COMPONENTS

sign	component description	value
L_{Ps}	primary series inductor	4.27 µH
C_{Pp}	primary parallel capacitor	255 nF
C_{Ps}	primary series capacitor	340 nF
L_P	primary self-inductances	42 µH
L_S	secondary self-inductances	42 µH
C_{Ss}	secondary series capacitance	340 nF
C_{Sp}	secondary parallel capacitance	255 nF
L_{Ss}	secondary series inductor	4.27 µH

Self-inductances of the primary and secondary side three phase coupler windings L_P, L_S, and the coupling coefficient k can be used to calculate the magnetizing inductance L_M as,

$$L_M = k\sqrt{L_P L_S} \tag{5}$$

Primary-side leakage inductance $L_{l,p}$ and secondary-side leakage inductance $L_{l,s}$ of the coupler can be acquired as,

$$L_{l,p} = L_P - L_M \tag{6}$$

$$L_{l,s} = L_S - L_M \tag{7}$$

Equivalent impedances of the primary-side, secondary-side, and the magnetizing branch, $Z_{P,eq}$, $Z_{S,eq}$, and $Z_{M,eq}$, respectively, can be stated by,

$$Z_{P,eq} = j\omega L_{11} + \left[\frac{1}{j\omega C_{11}} // \left(\frac{1}{j\omega C_{12}} + j\omega L_{l,p} + j\omega L_M\right)\right] \tag{8}$$

$$Z_{M,eq} = j\omega L_M \tag{9}$$

$$Z_{S,eq} = j\omega L_M + \frac{1}{n^2}\left[j\omega L_{l,s} + \frac{1}{j\omega C_{21}} + \left(\frac{1}{j\omega C_{22}} // j\omega L_{22}\right)\right] \tag{10}$$

where n is the turns ratio between primary and secondary coupler coils which is indicated as $n = \sqrt{L_S/L_P}$. Also, $\omega = \{2\pi f_{sw}\}$ is the angular operating frequency. The primary and secondary side phase voltage amplitudes V_P and V_S can be written by,

$$V_P = \frac{5}{3\sqrt{6}} V_{DC} \tag{11}$$

$$V_S = \frac{5}{3\sqrt{6}} V_{Battery} \tag{12}$$

The equivalent input resistance $R_{I,DC}$ and output resistance $R_{O,Battery}$ can be obtained as,

$$R_{I,DC} = \frac{2V_{DC}^2}{3\ P_I} \tag{13}$$

$$R_{O,Battery} = \frac{2V_{Battery}^2 \eta}{3\ P_O} \tag{14}$$

In a matrix form equation, the primary and secondary resonant network can be indicated as,

$$\begin{bmatrix} V_P \\ V_S \end{bmatrix} = \begin{bmatrix} Z_{P,eq} & -Z_{M,eq} \\ -Z_{M,eq} & Z_{S,eq} \end{bmatrix} \begin{bmatrix} I_P \\ I_S \end{bmatrix} \tag{15}$$

The system resonant frequency can be expressed by resonant compensation parameters as,

$$\omega_o = 1/\sqrt{L_{11}C_{11}} = 1/\sqrt{L_{22}C_{22}} = 1/\sqrt{(L_P - L_{11})C_{12}} = 1/\sqrt{(L_S - L_{22})C_{21}} \tag{16}$$

The voltage gain of the proposed system in charging and discharging mode can be extracted as,

$$|M_{V,charge}| = \left|\frac{V_S}{V_P}\right| = \left|\frac{\omega^2 L_M C_{Pp1}}{\left(1 - \left(\frac{\omega}{\omega_o}\right)^2 + j\omega C_{Ps1} R_{O,Battery}\right)\left(\frac{1}{C_{Ss1}} + j\omega L_S\right) + j\omega L_{S1} + R_{I,DC}}\right| \tag{17}$$

and

$$|M_{V,discharge}| = \left|\frac{V_P}{V_S}\right| = \left|\frac{\omega^2 L_M C_{Ps1}}{\left(1 - \left(\frac{\omega}{\omega_o}\right)^2 + j\omega C_{Pp1} R_{I,DC}\right)\left(\frac{1}{C_{Sp1}} + j\omega L_P\right) + j\omega L_{P1} + R_{O,Battery}}\right| \tag{18}$$

III. EXPERIMENTAL RESULTS

A laboratory test setup was assembled for experimental validation of the proposed system to demonstrate the functionalities of the bidirectional WPT system with step-up and step-down functionality. This system consists of primary and secondary side power electronics and identical couplers with 6 inches of airgap separation between coils. Wolfspeed/CREE CAS325M12HM2 1200 V / 325 A rated phase-leg SiC MOSFET power modules are used to form the converters in primary and secondary sides. In order to drive the three phase power modules, CREE CGD16HB62LP gate drivers are used for the system operation of the inverter. Liquid cooled MicroCool heatsinks are used with ethylene glycol and water mixture for the thermal management of power modules. TMS320F28335PGFA DSP module from Texas Instruments is used to control the presented bidirectional structure. The design specifications of the system are given in Table II.

TABLE II - EXPERIMENTAL DESIGN SPECIFICATIONS

sign	component description	value
V_{DC}	input voltage range	400 - 800 V_{DC}
$V_{Battery}$	battery output voltage	560 V_{DC}
P_O	rated output power	50 kW
l	magnetic air gap	6 inches
f_{SW}	step-up operating frequency	93.5 kHz
f_{SW}	step-down operating frequency	83.5 kHz
t_{dead}	dead time	600 ns

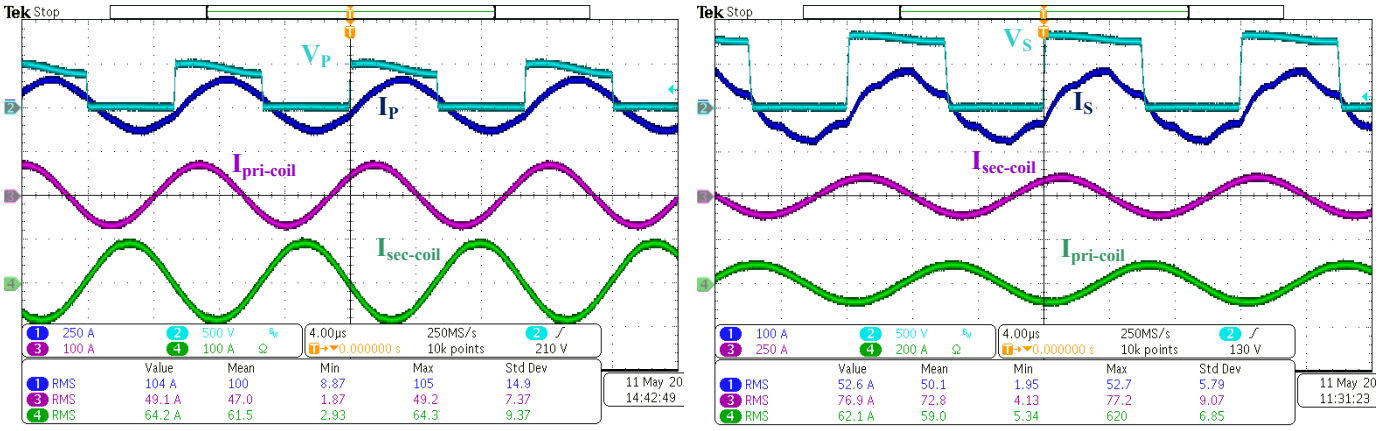

(a) (b)

Fig. 3. Experimental results of the bidirectional WPT system with resonant stage voltage and current waveforms at 50 kW power transfer for step-up configuration (a) and step-down configuration (b).

(a) (b)

Fig. 4. Power analyzer screenshots of the numeric experimental results of the bidirectional WPT systeme with 50 kW output power measurement for step-up configuration (a) and step-down configuration (b).

Experimental setup uses NHR 9300 battery emulators on the source and load sides to demonstrate the system performance with voltage step-up and step-down functionalities. For the energy circulation to charge and discharge the battery, the experimental results of the resonant circuit phase voltage and current signals are shown in Fig. 3 (a) and Fig. 3 (b) at 50 kW power transfer for the step-up and step-down formation, respectively.

The numerical power measurements of the system experimental results is presented by using Yokogawa WT1806E precision power analyzer as demonstrated in Fig. 4 (a) and 4 (b) for step-up and step-down configurations. As seen from the numerical results, the system overall efficiency is around 95.4 % for the step-up configuration at 50 kW power. Also, the experimental setup achieves an overall efficiency of 93.6% for the step-down operating mode with 50 kW power transfer as shown in Fig. 4 (b).

IV. Conclusions

This study introduces a bidirectional WPT system with voltage step-up and step-down functionalities with double-sided *LCC-LCC* resonant compensation with polyphase couplers having 6 inches airgap separation. The proposed system can be used for charging and discharging of ESSs, MESSs, EV batteries, etc. Theoretical analysis of the proposed system is presented and experimental results are provided for step-up and step-down operation modes. According to the experimental test results, when transferring power in step-up

mode, 95.4% overall system efficiency is achieved at 50 kW power transfer. In voltage step-down operating mode, 93.6% of overall efficiency is measured, while transferring 50 kW to the dc load terminals.

ACKNOWLEDGEMENTS

This project is funded by Oak Ridge National Laboratory's Laboratory Directed Research and Development (LDRD) Program's Transformational Energy Science and Technology (TEST) initiative with the project ID LOIS-9505. This research used resources available at the Power Electronics and Electric Machinery Research Center located at the National Transportation Research Center, a DOE EERE User Facility operated by the Oak Ridge National Laboratory (ORNL). The authors would like to thank the TEST Initiative Lead, Dr. Ilias Belharouak for his support of this work and his guidance. Authors also acknowledge the support and guidance of ORNL Sustainable Transportation Program Manager, Dr. Rich Davies, which is greatly appreciated.

REFERENCES

[1] O. C. Onar, G. -J. Su, E. Asa, J. Pries, V. Galigekere, L. Seiber, C. White, R. Wiles, and J. Wilkins, "20-kW bi-directional wireless power transfer system with energy storage system connectivity," in *Proc., IEEE Applied Power Electronics Conference and Exposition (APEC)*, pp. 3208-3214, March 2020, New Orleans, LA.

[2] E. Asa, J. Pries, V. Galigekere, S. Mukherjee, O. C. Onar, G. -J. Su, and B. Ozpineci, "A novel ac to ac wireless power transfer system for EV charging applications," in *Proc., IEEE Applied Power Electronics Conference and Exposition (APEC)*, pp. 1685-1690, March 2020, New Orleans, LA.

[3] E. Asa, K. Colak, D. Czarkowski, and B. Tamyurek, "Efficiency analysis of a bi-directional dc/dc converter for wireless energy transfer applications," in *Proc., IEEE Energy Conversion Congress and Exposition (ECCE)*, pp. 594-598, September 2015, Montreal, CA.

[4] K. Colak, E. Asa, D. Czarkowski, and H. Komurcugil, "A novel multi-level bi-directional dc/dc converter for inductive power transfer applications," in *Proc., Annual Conference of the IEEE Industrial Electronics Society (IECON)*, pp. 3827-3831, November 2015, Yokohama, Japan.

[5] E. Asa, O. C. Onar, J. Pries, V. Galigekere, and G. -J. Su, "A tradeoff analysis of series / parallel three-phase converter topologies for wireless extreme chargers," in *Proc., IEEE Transportation Electrification Conference & Expo (ITEC)*, pp. 1093-1101, June 2020, Chicago, IL.

[6] R. P. Twiname, D. J. Thrimawithana, U. Madawala, and C. A. Baguley, "A dual active bridge topology with a tuned CLC network," *IEEE Transactions on Power Electronics*, vol. 30, no. 12, pp. 6543-6550, Dec. 2015.

[7] B. Nguyen, D. Vilathgamuwa, G. Foo, P. Wang, A. Ong, U. Madawala, and T. Nguyen, "An efficiency optimization scheme for bidirectional inductive power transfer systems," *IEEE Transactions on Power Electronics*, vol. 30, no. 11, pp. 6310-6319, Nov. 2015.

[8] U. K. Madawala, M. Neath, and D. J. Thrimawithana, "A power frequency controller for bidirectional inductive power transfer systems," *IEEE Transactions on Industrial Electronics*, vol. 60, no. 1, pp.310-317, Jan. 2013.

[9] M. Moghaddami and A. I. Sarwat, "Single-phase soft-switched ac-ac matrix converter with power controller for bidirectional inductive power transfer systems," *IEEE Transactions on Industry Applications*, vol. 54, no. 4, pp. 3760-3770, July-Aug. 2018.

[10] S. Weerasinghe, U. K. Madawala, and D. J. Thrimawithana, "A matrix converter-based bidirectional contactless grid interface," *IEEE Transactions on Power Electronics*, vol. 32, no. 3, pp. 1755-1766, March 2017.

[11] E. Asa, O. C. Onar, V. P. Galigekere, G. -J. Su, and B. Ozpineci, "A novel bi-directional AC/DC - DC/AC wireless power transfer system for grid support applications," in *Proc., IEEE Applied Power Electronics Conference and Exposition (APEC)*, pp. 1197-1202, June 2021, Phonix, AZ.

[12] E. Asa, O. C. Onar, V. P. Galigekere, G. -J. Su, and B. Ozpineci, "A novel three-phase oak ridge AC / DC converter for wireless EV charger applications," in *Proc., IEEE Applied Power Electronics Conference and Exposition (APEC)*, pp. 437-443, June 2021, Phoenix, AZ.

[13] E. Asa, O. C. Onar, V. P. Galigekere, G. -J. Su, B. Ozpineci, "A novel three-phase Oak Ridge AC / AC converter for wireless mobility energy storage system (WMESS) connectivity," in *Proc., IEEE Applied Power Electronics Conference and Exposition (APEC)*, pp. 758-764, June 2021, Phoenix, AZ.

[14] E. Asa, O. C. Onar, V. P. Galigekere, R. Zheng, G. -J. Su, and B. Ozpineci, "A novel three phase Oak Ridge dc / ac converter for wireless grid tied applications," in *Proc., IEEE Transportation Electrification Conference & Expo (ITEC)*, pp. 1-6, June 2021, Chicago, IL.

[15] E. Asa, V. Galigekere, O. C. Onar, B. Ozpineci, J. Pries, and G. -J. Su,, "Wireless Power System," U.S. Patent 2021/0188106 A1, Jun. 24, 2021. Online Available: https://patents.google.com/patent/US20210188106A1. Accessed on: Nov. 24, 2021.